

## Doppler Imaging of the Onset of Turbulent Convection

J. P. Gollub and J. F. Steinman

*Physics Department, Haverford College, Haverford, Pennsylvania 19041, and Physics Department, University of Pennsylvania, Philadelphia, Pennsylvania 19104*

(Received 21 May 1981)

We demonstrate that large rectangular fluid layers have several essentially time-independent convective states above the critical Rayleigh number  $R_c$  in which the rolls align perpendicular to all lateral boundaries. The pattern is hence splayed and contains defects. Using real-time laser Doppler imaging, we show that the onset of time dependence at  $R_1 \cong 5R_c$  arises from a structural instability of the rolls which can be suppressed by a local heat source.

PACS numbers: 47.25.Gv, 47.20.+m

Recent experiments on the transition to turbulent Rayleigh-Bénard convection have left a number of fundamental questions unresolved. Although nonlinear stability theory<sup>1,2</sup> predicts a regime of time-independent convection above the critical Rayleigh number  $R_c$ , cryogenic thermal-transport measurements on circular layers of large but finite horizontal extent<sup>3,4</sup> show random time dependence surprisingly close to  $R_c$ , so that the existence of this regime is in doubt.

We have studied convective phenomena in a large rectangular fluid layer using a laser Doppler-scanning technique that permits the structure of the velocity field to be mapped in the horizontal plane. This mapping could be done in a time shorter than the characteristic times of velocity fluctuations near the onset, so that the space and time structure of one component of the velocity field  $\vec{v}(\vec{r}, t)$  could be recorded in digital form.

We find that: (a) A time-independent convective flow is often reached after a transient lasting a day or more. However, the convective rolls align perpendicular to all the lateral boundaries, thus forcing the pattern to contain defects. (b) The initial time dependence then occurs at  $R_1 \cong 5R_c$ , and is caused by a structural instability of the rolls, most likely the skewed varicose instability of Busse and Clever.<sup>1</sup> (c) The fluctuations can be suppressed by a line source of heat, and the amount of heat required is so large that thermal fluctuations can probably be ruled out as a source of random time dependence above  $R_1$ .

The experiments were performed in a  $10 \times 15 \times 0.5$  cm<sup>3</sup> layer bounded by copper plates. This was the largest size that permitted laser Doppler access through the lateral (Plexiglas) boundaries. The long-term thermal stability (several days) was always better than 1% of the critical temperature difference. The fluid was water at 70 °C where its Prandtl number is 2.5. The light-scattering techniques have been described else-

where.<sup>5</sup>

We found that stable flows do exist above  $R_c$ , but are strongly influenced by the lateral boundaries even for large layers. The rolls preferentially align with their axes perpendicular to the boundaries, causing the pattern to be splayed and to contain defects, where a roll of positive (or negative) vorticity ends. An example is shown in Fig. 1, where the dots are points at which the horizontal velocity is zero, i.e., points on the roll boundaries separating regions of opposite vorticity. This steady state was reached after a transient lasting for a day or so, a time comparable to the horizontal thermal diffusion time  $\tau_H = L^2/\kappa = 1.5 \times 10^5$  s, where  $L = 15$  cm and  $\kappa$  is the thermal diffusivity of the fluid.<sup>6</sup> A similar map made one day later can be superimposed on Fig. 1 to within a few percent of the roll spacing, except very near the defects.

The pattern of Fig. 1 is not unique; others are obtained (unpredictably) from different initial

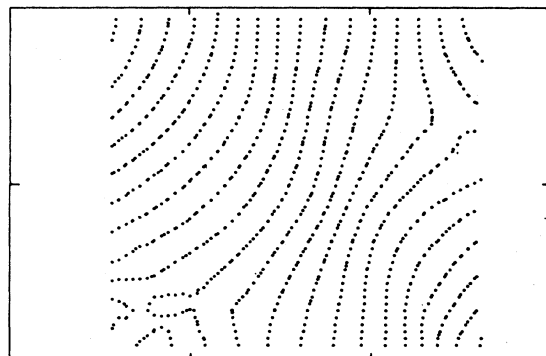


FIG. 1. Doppler map showing the structure of the velocity field above the midplane of the cell at  $R = 4.3R_c$ . The dots mark the roll boundaries. The pattern contains defects and the rolls are perpendicular to all four lateral boundaries in the time-independent steady state. (Part of the cell is outside the field of view.)

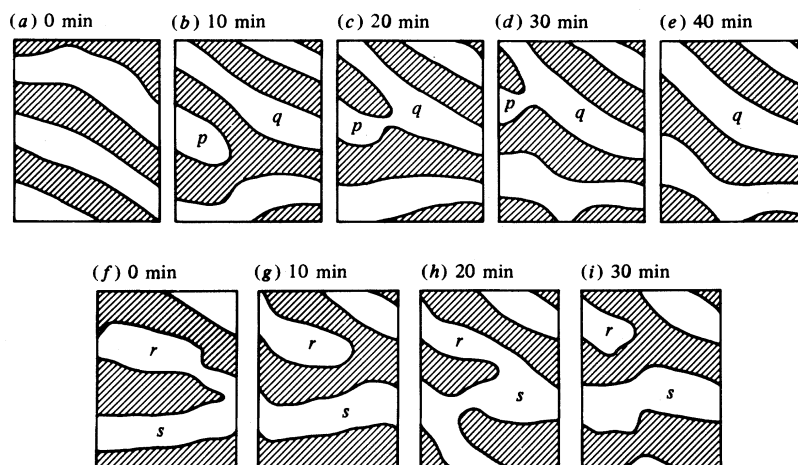


FIG. 2. Two sequences showing a portion of the velocity field at intervals of 10 min, at  $R = 5R_c$ . Shaded and unshaded regions have opposite vorticity. The rolls are clearly unstable.

conditions. Those with only a few defects (two is apparently the minimum number) tend to be stable after a long transient. On the other hand, patterns with many defects, which can be created by decreasing  $R$  from  $30R_c$ , continue to evolve very slowly even after a few days. In this respect, the behavior of the system in the interval  $R_c < R < 5R_c$  resembles that of a glass. The observation of relatively stable defects in a finite system is interesting in view of observations<sup>7</sup> and calculations<sup>8</sup> showing motion of defects at constant velocity in layers of very large extent.

Above  $R_1 = 5R_c$  (with a scatter of  $\pm 0.5R_c$ ) the local velocity begins to fluctuate slowly, with an amplitude that is greatest in the central region of the cell. The fluctuations are sufficiently slow that their space and time structure could be followed in detail by repetitive laser Doppler imaging. We scanned a portion of the center of the cell every ten minutes for runs lasting about ten hours, obtaining sixty images per run in digital form. While these images are not strictly instantaneous, they come reasonably close to this condition. Several sequences of images are shown in Fig. 2, where rolls circulating in one sense are shaded. In Fig. 2(b) the intrusion of a defect  $p$  is visible. In Fig. 2(c) it merges with a roll  $q$  of similar vorticity, and a new defect (now shaded) is expelled from the field of view. A second sequence begins in Fig. 2(f), where a roll labeled  $r$  is pinched off to form a defect, merges with region  $s$  [Fig. 2(h)], and is then separated once again [Fig. 2(i)]. These structural deformations are typical of the fluctuations just above  $R_1$ , though the activity is somewhat intermittent.

The power spectrum  $P(f)$  of the local velocity fluctuations is flat at low frequencies, and falls off as  $f^{-n}$  at "high" frequencies (but less than 0.025 Hz), where  $n = 4.1 \pm 0.4$ , independent of  $R$ , for  $5 < R/R_c < 10$ . The linewidth  $f_{\text{rms}}$  of the spectrum (square root of the second moment), whose inverse is a characteristic time scale, is approximately linear in  $R$  above  $R_1$  as shown in Fig. 3. However,  $f_{\text{rms}}$  may be finite just above  $R_1$ . Beginning at  $9R_c$ , intermittent oscillations appear in the local velocity records, and these are superimposed on the slower fluctuations already described. The spectrum then shows a broad peak at about 0.04 Hz which is initially rather well separated from the  $f^{-4}$  falloff associated with the slow fluctuations. This peak has been previously observed in thermal measurements by several workers,<sup>3,9</sup> and results from the oscillatory instability of Busse and Clever.<sup>1</sup> These two promi-

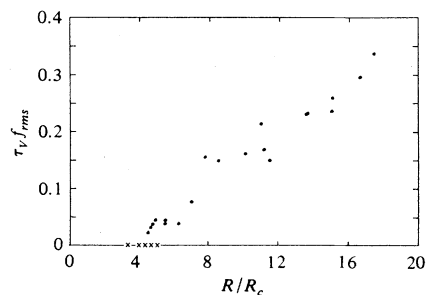


FIG. 3. Linewidth  $f_{\text{rms}}$  of the velocity power spectrum (scaled by  $\tau_V^{-1}$ , the inverse vertical thermal diffusion time) as a function of Rayleigh number. Crosses indicate no detectable time dependence.

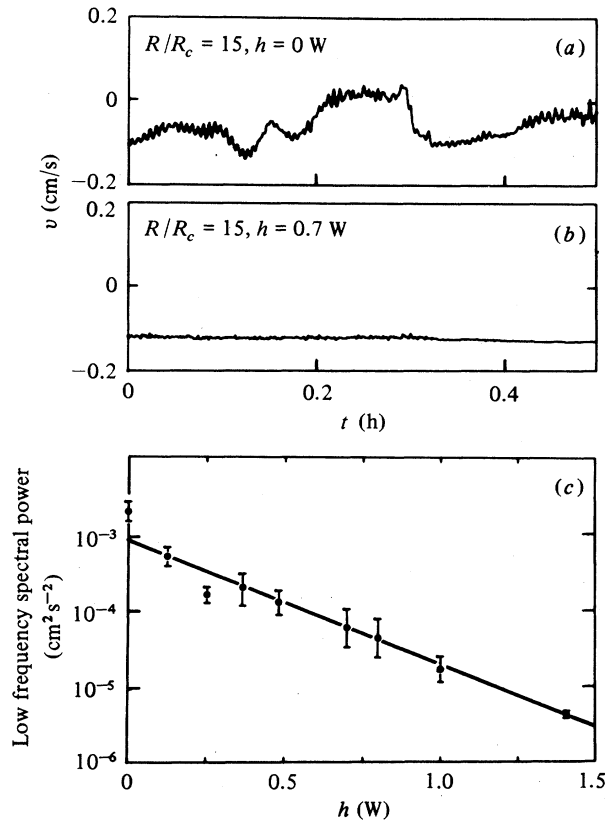


FIG. 4. A line source of heat  $h$  suppresses the low-frequency fluctuations almost completely. (a) Velocity near the wire when  $h = 0$ . (b) Velocity record when  $h = 0.7$  W. (c) Integrated spectral power below 0.025 Hz as a function of  $h$ , showing exponential suppression of the fluctuations.

nent spectral features associated with the transition to turbulence gradually merge as  $R$  is increased, but remain distinguishable even at  $R = 49R_c$ .

In order to obtain a quantitative measure of the strength of the fluctuations, we applied a line source of heat parallel to the short side of the cell using a Teflon-coated wire located 0.6 mm above the lower plate and 3 cm from the end of the cell. In the time-independent regime, a heat input  $h$ , small compared to the total heat flow through the cell, is sufficient to align the rolls with the wire over more than half the cell. In the time-dependent regime, the local velocity fluctuations are suppressed near the wire, as shown in Fig. 4. We characterize this suppression by the area  $A$  under the low-frequency portion ( $f < 0.025$  Hz) of the spectrum  $P(f)$ . We found that

$A$  varies exponentially with  $h$ :  $A \cong A_0 \exp(-h/h_0)$ , where the attenuation constant  $h_0 = 0.27$  W at  $R = 15R_c$ . For comparison,  $h_0$  is 14% of the heat flux carried per wavelength (two rolls). We find that  $h_0$  does not vary significantly with  $R$ , and that the suppression extends several wavelengths from the wire. Details of these experiments will be presented elsewhere.

Even a perfect roll structure is not expected to be stable up to the onset of the oscillatory instability, because of several other instabilities that dominate in various ranges of wave number and Prandtl number. These instabilities (cross roll, knot, and skewed varicose instabilities)<sup>1</sup> have no intrinsic time dependence in linear theory. At our Prandtl number and the observed roll wave number near  $R_1$  ( $2.7/d$ , where  $d$  is the layer depth), the skewed varicose instability is the first roll deformation that is predicted to occur as  $R$  is increased. Its predicted onset at  $R_{sv} = 4.7R_c$  is remarkably close to the observed onset of time dependence at  $R_1 = 5R_c$ , where Doppler imaging reveals the rolls to be unstable. Therefore, we identify this instability as the cause of the time dependence, a hypothesis that is consistent with a recent numerical simulation of the full Boussinesq equations by Siggia and Zippelius.<sup>10</sup> The fact that the fluctuations are robust, as indicated by the relatively large "pinning flux"  $h_0$ , seems to rule out thermal fluctuations<sup>11</sup> as playing a significant role in the time dependence above  $R_1$ .

The fluctuations studied (but not visualized) in circular layers of liquid helium by Ahlers and Behringer,<sup>3</sup> and Behringer *et al.*,<sup>4</sup> may be of similar origin, since the spectral shapes and variation of the characteristic frequency with  $R$  are quite similar. The skewed varicose instability is predicted to occur at much lower  $R$  for Prandtl numbers below 1, and is consistent with the onset of obvious time dependence at about  $2R_c$  in those experiments. The rare events observed more recently below  $2R_c$  by Ahlers and Walden<sup>11</sup> may be related to the residual slow time dependence that we find for patterns containing many defects.

We conclude that large rectangular convecting layers at moderate Prandtl number do have essentially time-independent convective states above  $R_c$ , but they contain defects.<sup>12</sup> The time dependence is noisy near its onset, and Doppler imaging shows that it arises from an instability of the rolls.

This work was supported by the National Science Foundation.

<sup>1</sup>F. H. Busse and R. M. Clever, *J. Fluid Mech.* **91**, 319 (1979).

<sup>2</sup>M. C. Cross, P. G. Daniels, P. C. Hohenberg, and E. D. Siggia, *Phys. Rev. Lett.* **45**, 898 (1980), and to be published.

<sup>3</sup>G. Ahlers and R. P. Behringer, *Phys. Rev. Lett.* **40**, 712 (1978), and *Prog. Theor. Phys. Suppl.* **64**, 186 (1978).

<sup>4</sup>R. P. Behringer, C. Agoste, J. S. Jan, and J. N. Shaumeyer, *Phys. Lett.* **80A**, 273 (1980); R. P. Behringer, J. N. Shaumeyer, J. S. Jan, C. Agosta, and C. A. Clark, to be published.

<sup>5</sup>J. P. Gollub and S. V. Benson, *J. Fluid Mech.* **100**, 449 (1980).

<sup>6</sup>A somewhat shorter time has been quoted by R. Krish-

namurti, *J. Fluid Mech.* **42**, 295 (1970). However, quantitative local measurements over times comparable to  $\tau_H$  were not feasible in that work.

<sup>7</sup>J. A. Whitehead, *J. Fluid Mech.* **75**, 715 (1976).

<sup>8</sup>E. D. Siggia and A. Zippelius, to be published.

<sup>9</sup>A. Libchaber and J. Maurer, *J. Phys. (Paris), Lett.* **9**, L369 (1978).

<sup>10</sup>E. D. Siggia, private communication.

<sup>11</sup>Thermal or other external fluctuations have been proposed as an explanation for early time dependence in moderate-aspect-ratio experiments by G. Ahlers and R. W. Walden, *Phys. Rev. Lett.* **44**, 445 (1980).

<sup>12</sup>Of course, it is still possible that a completely regular pattern might be stable if produced by controlled initial conditions.

## Propagation of an Intense Ion Beam Transverse to a Magnetic Field

S. Robertson, H. Ishizuka, W. Peter,<sup>(a)</sup> and N. Rostoker

*Department of Physics, University of California, Irvine, California 92717*

(Received 23 March 1981)

It has been verified experimentally that an intense, space-charge-neutralized ion beam having a dielectric constant  $\epsilon \gg 1$  will cross a transverse magnetic field undeflected. A polarization electric field  $\vec{E}$  is measured within the beam channel such that  $\vec{E} + (\vec{v}/c) \times \vec{B} = 0$ , where  $\vec{v}$  is the beam velocity and  $\vec{B}$  is the applied field. It is shown theoretically that  $\epsilon \gg (m_i/m_e)^{1/2}$  is required for the beam to enter the transverse field from a region with no field, where  $m_i$  and  $m_e$  are the ion and electron masses.

PACS numbers: 41.80.Gg, 07.77.+p, 52.30.+r, 52.50.Gj

We describe an experiment in which an intense, space-charge-neutralized ion beam passes undeflected through a strong transverse magnetic field. The penetration of an ion beam through a magnetic field has previously been reported.<sup>1,2</sup> Our observations are the first in which the polarization drift<sup>3</sup> has been clearly identified and measured as the mechanism of propagation for an intense ion beam. We also present a theoretical description of the motion which shows that a beam will propagate undeflected into a magnetic field from a field-free region only if  $\epsilon \gg (m_i/m_e)^{1/2}$ , where  $\epsilon$  is the static dielectric constant of the beam in the magnetic field,  $m_i$  is the ion mass, and  $m_e$  is the electron mass. The first theoretical description of the drift,<sup>3</sup> which applies to plasmas moving initially within a field, indicated a weaker condition ( $\epsilon \gg 1$ ) was necessary. It has been suggested that this mechanism could be used to propagate beams into magnetic fusion devices in order to drive currents or to provide supplementary heating.<sup>4,5</sup>

Experiments with dense plasmas ( $10^{13}$ – $10^{14}$

$\text{cm}^{-3}$ ) from coaxial guns<sup>6</sup> have verified a simple theoretical model<sup>3</sup> in which the Lorentz force acts on the ions and the electrons to create polarization layers on opposite surfaces of the plasma such that  $cE_y + v_x B_z = 0$ , where  $E_y$  is the polarization electric field,  $v_x$  is the beam velocity, and  $B_z$  is the applied field. This theory has been applied to plasmas in the form of a charge-neutralized ion beam ( $10^{10}$ – $10^{11}$   $\text{cm}^{-3}$ ) to determine three conditions necessary for the beam to cross a magnetic field.<sup>1,4,5,7</sup> First, the initial beam energy density should exceed the energy density necessary to set up the electric field. This is equivalent to  $\epsilon = 1 + \omega_{pi}^2/\Omega_i^2 \gg 1$ , where  $\omega_{pi}$  is the ion plasma frequency and  $\Omega_i$  is the ion cyclotron frequency.<sup>3</sup> Second, the thickness of the polarization layers should be much less than the beam radius  $r$ . This is equivalent to  $\rho_i/\epsilon \ll r$ , where  $\rho_i$  is the ion Larmor radius. Third, the potential at the positive surface of the beam should not exceed the ion accelerating potential. A negative potential cannot occur because the electrons in the beam have negligible energy and cannot